Applied Microbiology and Biotechnology (2018) 102:6959–6971
https://doi.org/10.1007/s00253-018-9138-7

BIOTECHNOLOGICALLY RELEVANT ENZYMES AND PROTEINS

EcXyl43 β-xylosidase: molecular modeling, activity on natural and artificial substrates, and synergism with endoxylanases for lignocellulose deconstruction

Ornella M. Ontañon[1,2] · Silvina Ghio[3] · Rubén Marrero Díaz de Villegas[1] · Florencia E. Piccinni[1,2] · Paola M. Talia[1,2] · María L. Cerutti[2,4] · Eleonora Campos[1,2]

Received: 14 March 2018 / Revised: 10 May 2018 / Accepted: 15 May 2018 / Published online: 6 June 2018

Abstract

Biomass hydrolysis constitutes a bottleneck for the biotransformation of lignocellulosic residues into bioethanol and high-value products. The efficient deconstruction of polysaccharides to fermentable sugars requires multiple enzymes acting concertedly. GH43 β-xylosidases are among the most interesting enzymes involved in hemicellulose deconstruction into xylose. In this work, the structural and functional properties of β-xylosidase EcXyl43 from *Enterobacter* sp. were thoroughly characterized. Molecular modeling suggested a 3D structure formed by a conserved N-terminal catalytic domain linked to an ancillary C-terminal domain. Both domains resulted essential for enzymatic activity, and the role of critical residues, from the catalytic and the ancillary modules, was confirmed by mutagenesis. EcXyl43 presented β-xylosidase activity towards natural and artificial substrates while arabinofuranosidase activity was only detected on nitrophenyl α-L-arabinofuranoside (pNPA). It hydrolyzed xylobiose and purified xylooligosaccharides (XOS), up to degree of polymerization 6, with higher activity towards longer XOS. Low levels of activity on commercial xylan were also observed, mainly on the soluble fraction. The addition of EcXyl43 to GH10 and GH11 endoxylanases increased the release of xylose from xylan and pre-treated wheat straw. Additionally, EcXyl43 exhibited high efficiency and thermal stability under its optimal conditions (40 °C, pH 6.5), with a half-life of 58 h. Therefore, this enzyme could be a suitable additive for hemicellulases in long-term hydrolysis reactions. Because of its moderate inhibition by monomeric sugars but its high inhibition by ethanol, EcXyl43 could be particularly more useful in separate hydrolysis and fermentation (SHF) than in simultaneous saccharification and co-fermentation (SSCF) or consolidated bioprocessing (CBP).

Keywords β-Xylosidase · GH43 · XOS · Hemicellulose · Synergism · Bioethanol

Introduction

The search for sustainable replacements of fossil fuels has focused the attention on the conversion of non-food lignocellulosic biomass into second-generation fuels along with higher value compounds, emerging the concept of biorefinery. Lignocellulosic feedstocks for these biorefineries include residues from agriculture, agro-industries, or wood and pulp and paper industries, rich in carbohydrate polymers (cellulose and hemicellulose) and polyphenols (lignin) together with other less abundant compounds, such as pectins (Jørgensen and Pinelo 2017). The complex arrangement of these molecules makes biomass highly recalcitrant, and therefore, the efficient enzymatic hydrolysis of polymers into monomeric sugars still remains the major challenge for current bioconversion technologies (Diogo et al. 2014).

Electronic supplementary material The online version of this article (https://doi.org/10.1007/s00253-018-9138-7) contains supplementary material, which is available to authorized users.

✉ Eleonora Campos
campos.eleonora@inta.gob.ar; eleonoracampos@yahoo.com

[1] Instituto de Biotecnología, CICVyA, Instituto Nacional de Tecnología Agropecuaria (INTA), Dr. N. Repetto y Los Reseros s/n, Hurlingham (1686), Buenos Aires, Argentina

[2] Consejo Nacional de Investigaciones Científicas y Técnicas (CONICET), Buenos Aires, Argentina

[3] Instituto de Suelos, CIRN, Instituto Nacional de Tecnología Agropecuaria (INTA), Buenos Aires, Argentina

[4] Fundación Instituto Leloir, IIBBA-CONICET, Avenida Patricias Argentinas 435, C1405BWE Buenos Aires, Argentina

Hemicelluloses are a heterogeneous class of polymers representing up to 35% of plant biomass, which may contain pentoses (D-xylose, L-arabinose), hexoses (D-mannose, D-glucose, D-galactose), and/or uronic acids (D-glucuronic, D-4-O-methylgalacturonic, and D-galacturonic acids). Xylan, the main hemicellulose component of hardwoods and herbaceous plants, is composed of a backbone chain of (1 → 4) linked β-D-xylopyranosyl units and α-L-arabinofuranose, β-D-glucopyranosyl uronic acid, and acetyl groups as substituents (Gírio et al. 2010). Therefore, xylan represents a rich source of D-xylose, a biotechnologically relevant sugar for bioethanol production and as a precursor of value-added products for industry. Because of its branched nature and heterogeneity, hemicellulose deconstruction to xylose requires the action of multiple enzymes, mainly endo 1,4-β-xylanases (EC 3.2.1.8) that cleave the internal linkages between β-D-xylopyranosyl units and β-xylosidases (EC 3.2.1.37), which attack xylooligosaccharides (XOS) releasing xylose (Diogo et al. 2014). The addition of auxiliary debranching enzymes, such as α-L-arabinofuranosidases (EC 3.2.1.55), β-glucuronidases (EC 3.2.1.139), acetyl xylan esterases (EC 3.1.1.72), and feruloyl esterases (EC 3.1.1.73), also favors the deconstruction (Dodd and Cann 2009).

GH43 family of glycosyl hydrolases comprises a range of enzymes necessary for the complete degradation of hemicellulose, particularly arabinoxylans. The main reported activities among this family are β-D-xylosidase, α-L-arabinofuranosidase, and endo-α-L-arabinanase (EC 3.2.1.99), but some xylanases, galactan 1,3-β-galactosidases (EC 3.2.1.145), exo-α-1,5-L-arabinofuranosidases (EC 3.2.1.-), and β-1,3-xylosidases (EC 3.2.1.72) have also been identified. Moreover, most of the characterized GH43 enzymes are dual-function β-D-xylosidase-α-L-arabinofuranosidases (Lagaert et al. 2014). In particular, GH43 β-xylosidases lead to inversion of the anomeric carbon configuration after the hydrolysis of short XOS to xylose, preventing, thus, the synthesis of long oligosaccharides by transglycosylation. This distinctive characteristic of GH43 regarding other β-xylosidases is desirable for bioethanol production, which requires fermentable sugars (Smaali et al. 2006). Therefore, it is interesting to evaluate new glycosyl hydrolases from this family not only as isolated biocatalyzers but also in combination with other hemicellulases. It is important to fully understand the activity mechanisms and interactions to rationally design minimal efficient enzymatic cocktails.

The aim of the current work was to thoroughly characterize the β-xylosidase EcXyl43, from *Enterobacter* sp. reported by our group (Campos et al. 2014) both molecularly and biochemically to unveil its mechanism of action and to evaluate its biotechnological application for hemicellulose deconstruction.

Materials and methods

Analysis of amino acid sequence and 3D structure modeling

A BLASTP analysis of EcXyl43 was performed against non-redundant protein sequences available in NCBI database (http://blast.ncbi.nlm.nih.gov/). For phylogenetic analysis, EcXyl43 was compared only to GH43 enzymes that had been previously characterized and whose activity had been confirmed. Amino acid sequences were retrieved from NCBI database and aligned using ClustalW program from MEGA software v6.0. The evolutionary history was inferred using the neighbor-joining method and the Poisson correction. The robustness of the tree topology was evaluated by calculating bootstrap values using 1000 replicates. Phylogenetic tree was built with MEGA v6.0 (Tamura et al. 2013).

Homology modeling by Iterative Threading ASSEmbly Refinement (I-TASSER) (Yang et al. 2015) was used to generate a three-dimensional model of EcXyl43 using multiple sequences of crystallized GH43 β-xylosidases as templates. Protein structures were retrieved from a PDB library (http://www.rcsb.org) by LOMETS server included in I-TASSER, which generates 3D models by collecting high-scoring target-to-template alignments. LOMETS is a meta-server containing multiple threading programs that can generate thousands of template alignments. I-TASSER only uses the templates of the highest significance in the threading alignments. The following PDB templates were selected by LOMETS to construct the model: 3c2uA, 2exiA, and 1yifA. The fragments from templates with the highest significance in the threading alignments were re-assembled into a full-length model.

The final model resulted from a second simulation round which removed the steric clashes and refined the global topology (https://zhanglab.ccmb.med.umich.edu/I-TASSER). It was validated based on C-score (confidence score), TM-score (template modeling score that indicates the similarity between two protein structures), and RMSD (root-mean-square deviation of atomic positions between the superimposed proteins). C-score is typically in the range [−5, 2], wherein a higher score reflects a model of better quality. TM-score has the value between [0, 1], where 1 indicates a perfect match between two structures (Roy et al. 2010). The quality of the model was further validated by ProSA analysis (https://prosa.services.came.sbg.ac.at/prosa.php).

Functional analysis was conducted by COACH within I-TASSER, which included prediction of the protein-ligand

binding site. Model manipulation and imaging were performed using Chimera software (Pettersen et al. 2004).

ConSurf server was used to evaluate the conservation score of each single residue according to a multiple sequence alignment of the closest 150 similar sequences by CSI-BLAST (http://consurf.tau.ac.il).

Cloning of the two modules of EcXyl43

The catalytic (939 bp) and ancillary (672 bp) modules of EcXyl43 were amplified independently by PCR using pET28a-EcXyl43 plasmid as a template (Campos et al. 2014) and the pair of primers 43FBam/Ri43Xho and FiMANhe/43RXho, respectively (Table 1). The length of each module was determined based on Pfam location of catalytic (glycosyl hydrolase family 43) and ancillary modules (DUF1349 superfamily) and previous reference of other GH43 (Morais et al. 2012).

The amplified fragments were cloned in pET28a vector (previously digested with the corresponding restriction enzymes) for His-tag N-terminal fusion.

PCR mutagenesis

Site-directed mutagenesis reactions (Asp14 by Ala, Trp73 by Gly, Phe507 by Ala, and Phe511 by Ala) were performed using the Quickchange XL kit (Agilent Technologies, Santa Clara, CA), with pET28a-EcXyl43 plasmid as template. All the mutated residues were selected because of their high conservation within the family GH43 (around 100% according to the analysis performed with ConSurf). In particular, Asp14, Trp73, and Phe507 were predicted as part of the active site, while Phe511 would be located in the hinge interphase of both modules.

Highly purified pairs of primers that contained the desired mutations and annealed to opposite strands were designed (Table 1), according to the manufacturer's recommendations. Resulting plasmids were sequenced to confirm the desired mutation (and to confirm that no additional mutations were introduced) and used for transforming competent cells.

Protein expression and purification

E. coli BL21 (pLys) competent cells were transformed with the recombinant plasmids (pET28a-ancillary module, pET28a-catalytic module or pET28a-EcXyl43D14A, W73G, F507A, and F511A mutants). Recombinant clones were selected for protein expression and purification, along with EcXyl43 wild type, as previously described (Campos et al. 2014). Briefly, protein expression was induced with 1 mM IPTG for 16 h at 37 °C. After cell lysis, recombinant proteins were purified in the soluble fraction by immobilized metal affinity chromatography (IMAC) with Ni-NTA agarose resin (Qiagen), using 50 mM NaH_2PO_4, 300 mM NaCl, 250 mM imidazole pH 8.0 as elution buffer (QIAexpressionist). Purified proteins were conserved at 4 °C. For static light scattering (SLS) experiments, purified EcXyl43 was concentrated by ultrafiltration at 4 °C using a centricon column (3-kDa cutoff, Millipore) and further purified by size exclusion chromatography (SEC) using a Superdex 200 GL 10/300 column (GE Healthcare) equilibrated with buffer 50 mM Tris/HCl pH 8.0 and 300 mM NaCl.

SLS measurements

The average molecular weight of EcXy143 (450 μg) was determined with a Precision Detector PD2010 90° light scattering instrument connected in tandem to a LKB 2142

Table 1 PCR primers for the development of EcXyl43 mutants

Reaction	Primer	Sequence	T annealing (°C)
Amplification of catalytic module	43FBam Ri43Xho	5′GGATCCATGGAAATCACTAACCCGATACT 3′ 5′CTCGAGTTACAGCTGCGCGTGCTTACC 3′	55
Amplification of ancillary module	FiMANhe 43RXho	5′ GCTAGCACCGTGAAAGGCCCGCAG 3′ 5′CTCGAGTTATCAGGCCGGCTCGTAGGTGAAGTAG 3′	55
Directed mutagenesis D14A	D14Afor D14Arev	5′GCTTCAACCCGGCCCCGTCCCTGTG 3′ 5′CACAGGGACGGGGCCGGGTTGAAGC 3′	60
Directed mutagenesis W73G	W73Gfor W73Grev	5′CTCCGGCGGTATCGGGGCGCCGT 3′ 5′ACGGCGCCCCGATACCGCCGGAG 3′	60
Directed mutagenesis F507A	F507Afor F507Arev	5′GGGCGCGGCTTCGCCACCGGCGCGTTTGTGGG 3′ 5′CCCACAAACGCGCCGGTGGCGAAGCCGCGCCC 3′	60
Directed mutagenesis F511A	F511Afor F511Arev	5′GGCTTCTTCACCGGCGCGGCTGTGGGGCTGCACTGC3′ 5′GCAGTGCAGCCCCACAGCCGCGCCGGTGAAGAAGCC 3′	60

differential refractometer and to a 486 Absorbance Detector (Waters), set at 280 nm. The SEC chromatographic run was performed in the conditions described above at a flow rate of 0.4 ml/min at 20 °C. The molecular weight of the sample was calculated relating its 90° SLS and RI signals and comparing this value with the one obtained for bovine serum albumin as standard (MW 66.5 kDa) using the Discovery32 software.

Enzymatic assays

β-Xylosidase and arabinofuranosidase activities were assayed using 4-nitrophenyl-β-D-xylopyranoside (pNPX) and 4-nitrophenyl-α-L-arabinofuranoside (pNPA) (SIGMA), respectively. Reactions of 0.1 ml contained 2.5 mM of substrate prepared in 50 mM citrate/phosphate buffer ($I = 0.3$ M) pH 6.5 and the properly diluted enzyme solution. Mixtures were incubated at 40 °C during 20 min, and the reaction was stopped by adding 2% Na_2CO_3 (0.25 ml). The released p-nitrophenol (pNP) concentration was calculated according to a standard curve measuring the absorbance at 410 nm. Enzyme activities were expressed as U/mg of protein. One unit (U) of β-xylosidase or α-arabinofuranosidase activity was defined as the amount of enzyme that liberates 1 μmol pNP per minute at the assayed conditions.

β-xylosidase activity on XOS was performed in 40-μl reaction mixtures containing xylobiose (X2), xylotriose (X3), xylotetraose (X4), xylopentaose (X5), or xylohexaose (X6) (1.25–20 mM) prepared in 50 mM citrate/phosphate buffer (I = 0.3 M) pH 6.5. Enzymatic hydrolysis by EcXyl43 (0.1 mg/ml) was carried out at 40 °C during 30 min, stopped by boiling, and cleared by centrifugation (10,000*g*, 10 min). Xylose concentrations were determined using an enzyme coupled spectrophotometric assay (Megazyme Xylose-kit). The software GraphPad Prism was employed to identify the best kinetics model for each substrate and to calculate the kinetic parameters K_{cat}, K_M, and Vmax. Additional experiments were performed to evaluate the hydrolysis of XOS over time. For this, an initial concentration of 1.5 mg/ml of each substrate and 0.5 mg/ml of enzyme was used. The reactions were stopped after 30, 60, and 120 min and the xylose released was measured as previously detailed. The hydrolysis profiles of XOS over time were visualized by thin layer chromatography (TLC).

Xylanase and arabinofuranosidase activities were assessed on 0.5% beechwood xylan (Sigma) and medium viscosity wheat arabinoxylan (Megazyme) prepared in 100 mM citrate buffer pH 6.0. EcXyl43 was added in a final concentration of 0.25 mg/ml, and the reactions were performed at 40 °C during 1, 4, and 16 h. Insoluble xylan was prepared by boiling beechwood xylan for 30 min in distilled water and recovering the pellet by centrifugation three times to remove soluble sugars and after that dry weight was determined (Morais et al. 2012). The reducing sugars released by enzymatic hydrolysis reactions were measured using the DNS assay (Miller 1960) with xylose as standard. Xylose and arabinose were quantified by HPLC.

For reactions performed with natural substrates, one unit (U) of xylanase, β-xylosidase, or arabinofuranosidase activity was defined as the amount of enzyme that releases 1 μmol of xylose or arabinose per minute at the assayed conditions.

Thermal stability

For determination of thermal stability, the enzyme was pre-incubated at 40, 45, or 50 °C at different time intervals (5 min to 96 h) in 50 mM citrate/phosphate buffer ($I = 0.3$ M) pH 6.5. After ice cooling during 10 min, the residual activity on pNPX was measured according to the standard assay. Half-life ($t_{1/2}$) value of thermal inactivation was calculated by the equation $t_{1/2} = \ln 2/K_d$, where K_d is the inactivation rate constant obtained from the slope by plotting ln (residual activity) vs time.

Effect of divalent cations, monomeric sugars, and ethanol

Divalent cations (1–10 mM), ethanol (1–20%), and monosaccharide sugars (xylose, glucose, and arabinose) were added to the standard reaction mixture containing pNPX. Then, the residual β-xylosidase activity was calculated according to control conditions without additives, considered as 100%.

The extent of monosaccharide inhibition was determined by adding 100 mM xylose, glucose, or arabinose to the standard reaction with increasing concentrations of pNPX (2.5–20 mM). Kinetic parameters, Vmax, K_M, and Ki were calculated by curve fitting the data to the Michaelis-Menten model using GraphPad Prism 5 and the eqs. 1 and 2

$$K_M\,(ap) = K_M + \left(K_M{}^{*}(I/Ki)\right) \quad (1)$$

$$Vmax\,(ap) = Vmax/(1 + (I/Ki)) \quad (2)$$

where K_M (ap) and Vmax (ap) are the kinetic constants obtained in the presence of competitive or non-competitive inhibitors and Ki (inhibition constant) represents the sugar concentration at which 50% inhibition is observed. I is the inhibitor concentration (mM).

Addition of EcXyl43 to xylanases for hemicellulose deconstruction

The additive effect of EcXyl43 with endoxylanases in hemicellulose deconstruction was evaluated using beechwood xylan (0.5%) and pre-treated lignocellulosic biomass (2%) as substrates.

Beechwood xylan was incubated during 1 h in the presence of recombinant endoxylanases GH10XynA or GH11XynB from *Paenibacillus* sp. A59 (Ghio et al. 2018) alone and/or

combined with EcXyl43. Biomass hydrolysis was performed using extruded wheat straw (EWS) and each recombinant xylanase plus EcXyl43 for 24 h. All reactions were carried out at pH 6.0 and 45 °C and each enzyme was added to a final concentration of 0.25 mg/ml. Xylose released was quantified by HPLC, and the results obtained in reactions with and without EcXyl43 were statistically compared.

Visualization and quantification of hydrolysis products

XOS hydrolysis profiles were visualized by TLC in silica gel plates, using butanol-acetic acid-water (2:1:1) as solvents and revealed by water/ethanol/sulfuric acid (20/70/3) 1% orcinol solution, over flame.

Soluble sugars were quantified by HPLC, using a Rezex RPM-Monosaccharide column (Phenomenex) (80 °C, flow 0.6 ml/min), with a RI detector at 35 °C. Xylohexaose, xylopentaose, xylotetraose, xylotriose (Megazyme), xylobiose, xylose, and arabinose (Sigma) were used as chromatography standards.

Statistical analyses

All the assays were carried out at least in triplicate. Statistical analyses were conducted using GraphPad Prism 5. Unpaired *t* test and variance analysis were performed with a probability level of < 0.05.

GenBank accession number

The amino acid sequence of EcXyl43 was deposited in GenBank database with the accession number AFZ78871.

Results

Phylogenetic analysis and structure prediction of EcXyl43

Based on BLASTP analysis, the amino acid sequence of EcXyl43 showed 99% identity, with 100% coverage, with uncharacterized GH43 β-xylosidases from *E. cloacae* complex (WP_047062263; WP_047731179), but it presented less than 60% sequence identity with GH43 enzymes with known activity or solved 3D structure (available PDB). The phylogenetic analysis of EcXyl43 was performed against previously characterized GH43 since some authors suggested that the enzymes from this family with identical biological function may group together in phylogenetic clades (Lagaert et al. 2014). In this sense, EcXyl43 grouped with GH43 β-xylosidases and α-L-arabinofuranosidases, presenting the closest relationship with enzymes from *Bifidobacterium adolescentis* (BAF39209, 51% identity), *Bifidobacterium animalis* (ADC85541, 49% identity), *Lactobacillus brevis* (ABJ65333, 48% identity), and *Weisella* sp. (ALB06585, 47% identity) (Fig. 1).

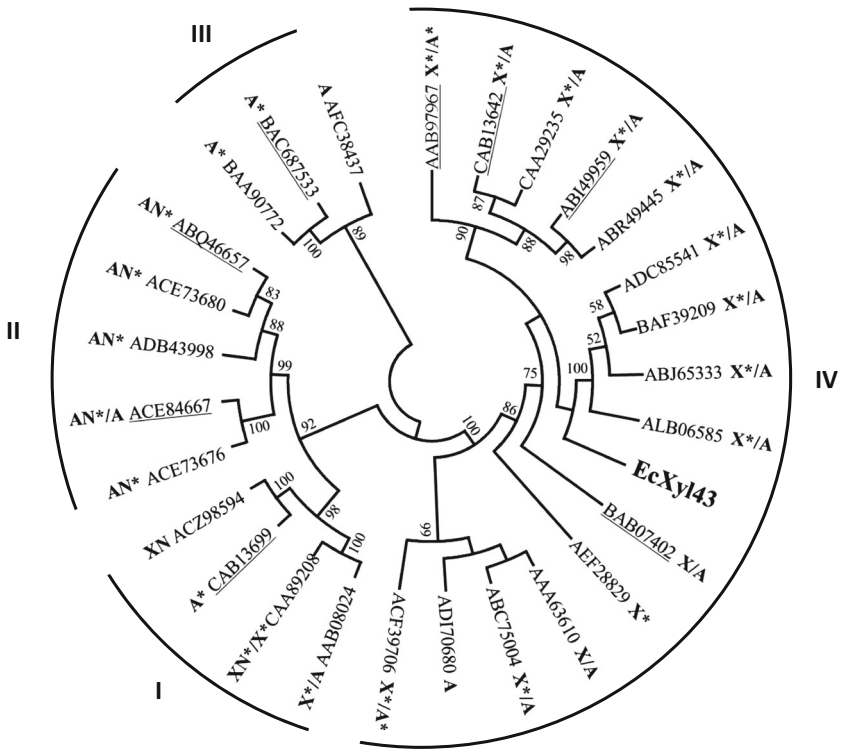

Fig. 1 Evolutionary relationships of EcXyl43 and characterized glycosyl hydrolases from family 43. Different specificity clusters are divided into four groups (I-IV). Enzyme activities are abbreviated as X: β-D-xylosidase; A: α-arabinofuranosidase; AN: arabinanase; XN: xylanase. The activities that were confirmed on natural substrates are indicated with asterisks. The proteins with known crystallographic structure are underlined

A unique 3D model of EcXyl43 was built based on multiple crystallographic structures of related GH43 proteins. The model accuracy was supported by a high C-score (1.99 of a maximum score of 2), and the β-xylosidase SXA from *Selenomonas ruminantium* (PDB: 3c2uA) was the most similar structural analog with a TM score of 0.99 (maximum 1) and an RSMD of 0.31. PRoSA analysis resulted in a Z-score of − 8.47, which is in line with Z-score of crystalized proteins of the same molecular weight, additionally supporting the high quality of the obtained model. The predicted model (Fig. 2) had an N-terminal five-bladed β-propeller domain (Met1-Lys319), typical of catalytic domains of β-xylosidases from GH43, connected by a linker (Val320–Ser330) to an ancillary C-terminal β-sandwich domain of undefined function (Trp331–Val536). The active site would be located in the center of the five-bladed β-propeller, and the residues Asp14, Glu186, and Asp127 were identified as the conserved catalytic triad. The sequence alignment and structural analysis revealed the presence of conserved possible xylobiose binding residues (Asp14, Ser29, Phe31, Trp73, Ala74, Phe126, Asp127, Trp145, His154, Glu186, Thr206, His248, Arg289, and Phe507) involved in hydrogen bond formation and stacking interactions (Fig. 3). Although the catalytic site was entirely located in the GH43 catalytic module, the structural model predicted Phe507, from the ancillary module, to be inserted in the catalytic domain through a long loop (Ser497-Ala510). Also, six residues probably involved in binding to Ca^{+2} were identified (Fig. S1), three of them located in the catalytic module (Ser16, Pro128, His248) and three in the ancillary module (Asp334, Gly363, and Asp529). Gel electrophoresis (Fig. S2) and SLS analyses confirmed that EcXyl43 formed oligomeric structures in solution. The average MW estimated by SLS for the main peak was 259.8 kDa (Fig. 4), consistent with the theoretical MW of a tetramer.

Both modules were expressed independently and purified in the soluble fraction (Fig. S2) with a molecular weight consistent with the theoretical (38.8 KDa for the catalytic module and 30.4 KDa for the ancilliary module), and their activity was evaluated. None of them showed β-xylosidase activity when pNPX was used as a substrate. Moreover, the enzymatic activity was not recovered by co-incubation of both modules, discarding possible non-covalent association, contrary to a GH43 from *Thermobifida fusca* (Morais et al. 2012).

Similarly, site directed mutations D14A, W73G, and F507A completely annulled the activity. These results supported the identification of the catalytic residues and demonstrated that the enzyme must be intact to be active since it requires amino acids from both modules to carry out the hydrolysis. Phe511, a highly conserved residue located in the hinge between the two modules but not predicted to be part of the catalytic pocket, was also mutated. Mutant F511A maintained the same β-xylosidase activity and kinetic parameters as the wild type, supporting that this residue is not critical for enzymatic activity (Fig. S3).

Substrate specificity of EcXyl43

We had previously demonstrated that EcXyl43 had β-xylosidase activity on pNPX and X2 (Campos et al. 2014). To further characterize substrate specificity, activity on several natural and artificial substrates was evaluated (Table 2, Fig. S4). EcXyl43 showed β-xylosidase activity on pNPX (1.52 U/mg) and short XOS (X2 to X6). EcXyl43 also

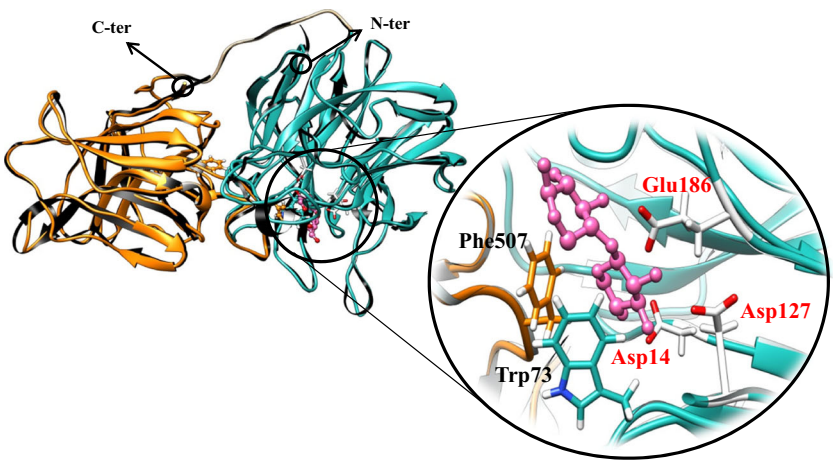

Fig. 2 Homology model of EcXyl43 obtained with I-TASSER server. The polypeptide chain is represented in orange (C-terminal ancillary domain) to turquoise (N-terminal catalytic domain) and the linker region is in gray. The active site is highlighted and the three catalytic amino acids (Asp14-Asp127-Glu186) are colored in white and red. Trp73 (catalytic module) is shown in turquoise and Phe507 (ancillary module) is shown in orange. The 3D structure of the most similar structural analog (PDB: 3c2u) is indicated in black. The interaction topology with xylobiose (in magenta) was suggested by COACH after structural alignment with the molecular model of PDB: 2exk

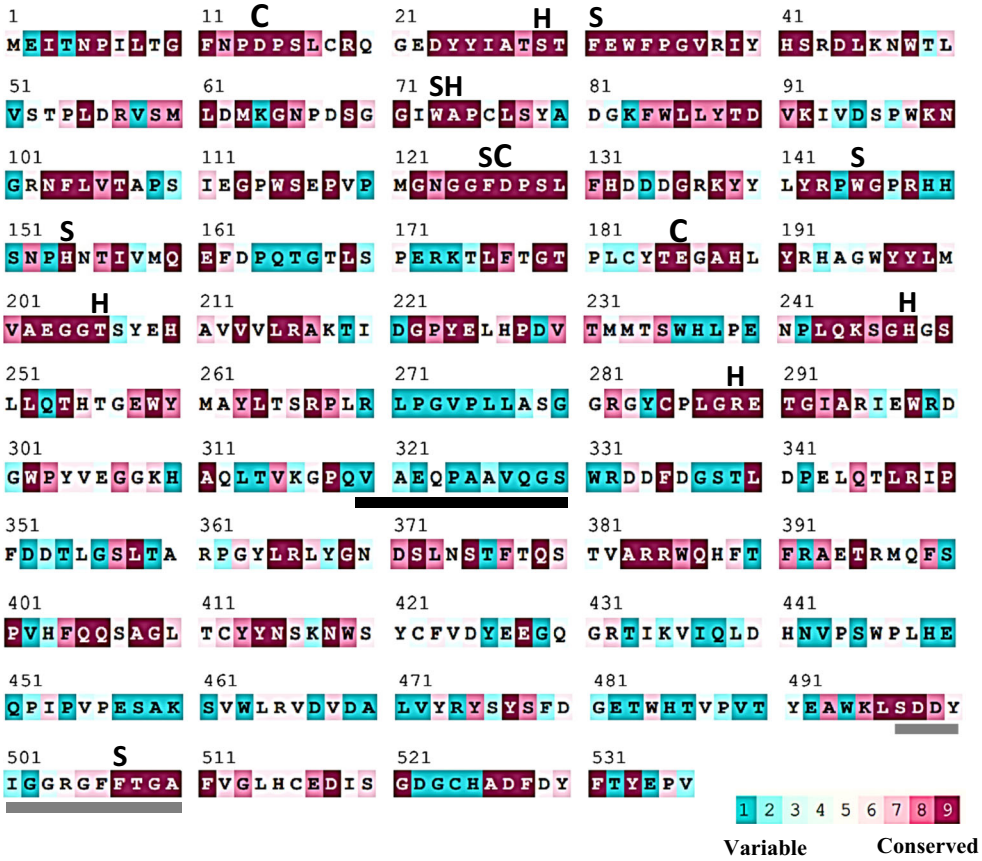

Fig. 3 ConSurf analysis for EcXyl43. The amino acids are colored by their degree of conservation according to a color-coding scale, with turquoise-to-violet indicating variable-to-conserved. The active site residues are denoted with letters: catalytic triad (C) and substrate binding residues through hydrogen bonding (H) and hydrophobic or stacking interactions (S). The linker region between the two domains: catalytic N-terminal (1–319) and ancillary C-terminal (331–536) is underlined in black. The gray line indicates the amino acids from the C-terminal domain inserted as a loop into the catalytic domain

displayed low levels of α-arabinofuranosidase activity on pNPA (0.04 U/mg). This last finding suggested that the enzyme is a true β-D-xylosidase, with a minor α-L-arabinofuranosidase side activity. However, neither xylose nor arabinose were released from wheat arabinoxylan (38% substitution), indicating either lack or very low arabinofuranosidase activity on arabinose (1 → 2) and (1 → 3) substituted xylan. Some activity was detected on soluble XOS present in beechwood xylan (0.07 U/mg, by reducing sugar quantification), with xylose being a main reaction product with a significant increase along prolonged time (16 h) (Fig. S5). However, no activity was observed on the insoluble fraction of xylan.

The kinetic constants for XOS hydrolysis were calculated as the rate of xylose released from increasing molar concentrations of X2 to X6. Data was fitted by nonlinear regression to the Michaelis-Menten model (Fig. 5a). The turnover number (K_{cat}) increased from X2 to X4, reaching a constant value for substrates of polymerization degree (DP) > 4. The K_M values revealed a higher affinity of the enzyme for X5 and X6. Additionally, the increased catalytic efficiency (K_{cat}/K_M) from X2 to X6 suggested that EcXyl43 had an efficient β-xylosidase activity against longer XOS (Fig. 5b).

The XOS hydrolysis profiles along the time were visualized by TLC (Fig. 5c). EcXyl43 released xylose as a main reaction product, which was not transferred to the

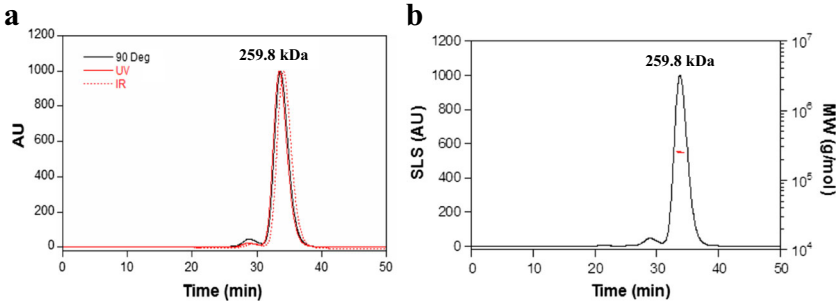

Fig. 4 SEC-SLS analysis of EcXyl43. Normalized light scattering at 90° (black line), UV absorption at 280 nm (red line) and IR (red dotted line) signals of the elute (**a**). The trace of the calculated MW is presented in red (**b**). The experimental MW value is indicated above the peak

Table 2 Specific activity of EcXyl43 towards pNP-monosaccharides, XOS, and xylan

Substrate	Product measured	Specific activity (U/mg protein)
pNPX[a]	pNP	1.52 ± 0.13
pNPA[a]	pNP	0.04 ± 0.00
Xylobiose[a]	Xylose	0.16 ± 0.01
Xylotriose[a]		0.31 ± 0.01
Xylotetraose[a]		0.60 ± 0.02
Xylopenatose[a]		1.03 ± 0.12
Xylohexaose[a]		1.10 ± 0.11
Beechwood glucuronoxylan[b]	Total soluble sugars	0.07 ± 0.02
	Xylose	0.08 ± 0.01
Wheat arabinoxylan[b]	Total soluble sugars	0.05 ± 0.01
	Xylose	None

[a] 2.5 mM
[b] 0.5%

substrate to form XOS of higher DP, similarly to other exo-acting β-xylosidases.

The reaction performance was similar for X2 to X4 when they were used at the same concentration (1.5 mg/ml), achieving an almost complete hydrolysis to xylose after 120 min (Fig. 5d). In accordance with the above mentioned kinetic results, xylose was released from X5 and X6 more efficiently at short reaction times with respect to low DP XOS.

Synergism with endoxylanases

In second-generation ethanol production, endoxylanase activity is crucial in enzymatic cocktails for biomass deconstruction, not only to obtain C5 sugars but most importantly to improve accessibility of cellulases to cellulose (Selig et al. 2008). Xylo-oligomers can result in inhibition of both endoxylanases and cellobiohydrolases, and therefore, it is important to minimize XOS in hydrolysis reactions.

The cooperative action of EcXyl43 with two recombinant endoxylanases from families GH10 and GH11, which have different activity mechanisms towards xylan (Ghio et al. 2018), was tested on the hydrolysis of beechwood xylan and EWS.

The combined application of EcXyl43 and GH10XynA released the highest amount of xylose from xylan (around 238 mg/g) with a 42% increase over the hydrolysis carried out only by the endoxylanase (Fig. 6a, c). Meanwhile, the

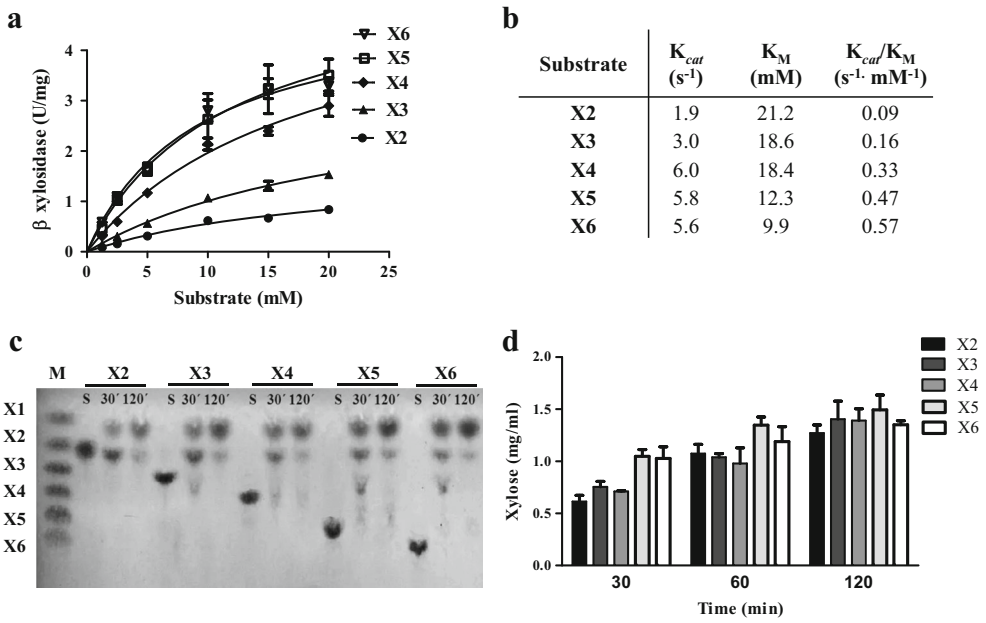

Fig. 5 Activity of EcXyl43 on short xylooligosaccharides. Nonlinear regressions to the Michaelis–Menten equation **(a)** and kinetic constants **(b)** for the hydrolysis of X2 to X6 into xylose (X1). The hydrolysis products along the time visualized by TLC are shown in **c**, where M is a mixture of X1 to X6 used as standard and S is the substrate control. The concentration of X1 released from 1.5 mg/ml substrate after 30, 60, and 120 min is plotted in **d**. All assays were performed at 40 °C, pH 6.5 with 0.1 mg/ml **(a**, **b)** and 0.5 mg/ml **(c**, **d)** of enzyme. Error bars represent standard deviations

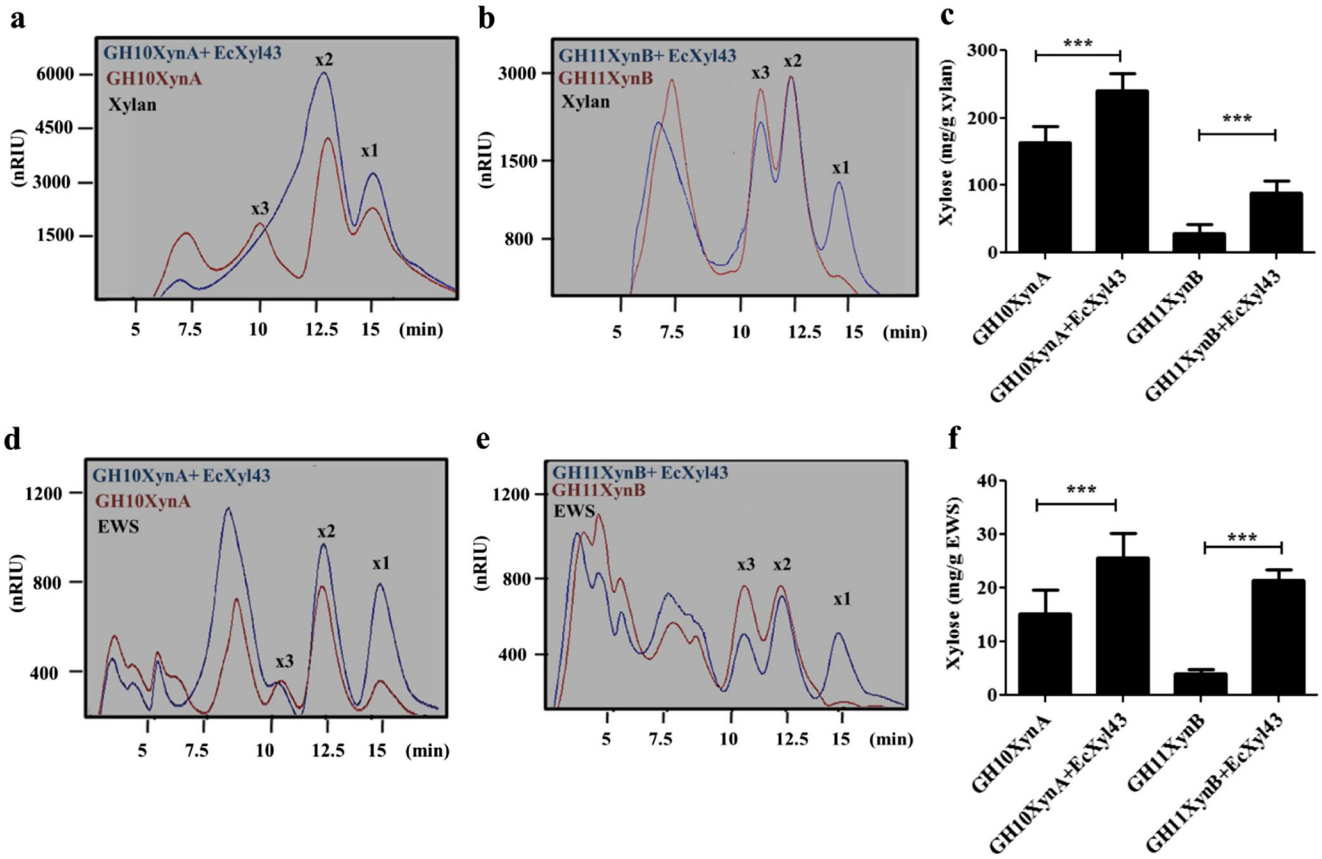

Fig. 6 Synergism of EcXyl43 with xylanases. HPLC hydrolysis profiles by EcXyl43 in combination with GH10XynA (**a**, **d**) or GH11XynB (**b**, **e**), of xylan (**a**, **b**) and extruded wheat straw (EWS) (**d**, **e**). HPLC was run using xylose (X1), xylobiose (X2), and xylotriose (X3) as standards. The concentration of xylose released from xylan (**c**) and EWS (**f**) corresponds to the average of two independent assays with three replicates for each condition. Asterisks indicate significant differences ($p < 0.001$) between the two analyzed conditions. Error bars represent standard deviations

addition of EcXyl43 to GH11XynB markedly enhanced xylan hydrolysis to xylose, since GH11XynB activity products were only XOS of DP > 2 and an almost negligible concentration of the monomer (Fig. 6b, c). The observed synergistic effect can be attributed to the formation of short XOS by endoxylanases, further hydrolyzed by EcXyl43.

Similar results were obtained for the hydrolysis of EWS (Fig. 6d–f). The addition of EcXyl43 significantly increased the conversion to xylose, with a maximal yield achieved by the combination of EcXyl43 with GH10XynA (25.5 mg xylose/g biomass) (Fig. 6f). The lower conversion efficiency to xylose from biomass compared to xylan could be related either to a limited enzyme access to the hemicellulosic polymer or the biomass recalcitrance generated by the pre-treatment.

Thermal stability and tolerance to divalent cations, monomeric sugars, and ethanol

The search for novel enzymes suitable for industrial lignocellulose deconstruction requires not only high specific activities but also thermal stability (as hydrolysis processes range from 24 to 72 h), low inhibition by end products, and tolerance to inhibitory compounds that can be produced during pre-treatment. For simultaneous saccharification and fermentation (SSF, SSCF) or consolidated bioprocess (CBP) applications, activity at lower temperatures and tolerance to ethanol are also desirable.

Optimal activity conditions of EcXyl43 were previously defined as 40 °C and pH 6.5 (Campos et al. 2014). At these conditions, the enzyme remained active even after 96 h of incubation and exhibited a half-life of 58.7 h (Table 3).

Table 3 Thermal stability of EcXyl43 at different temperatures and in the presence of Ca^{+2}

T (°C)	Ca^{+2} (mM)	$t_{1/2}$ (h)	K_d (h^{-1})
40	–	58.73	0.01
45	–	5.71	0.12
50	–	0.14	4.77
50	1	0.64	1.08
50	5	0.60	1.15
50	10	0.51	1.33

However, the stability decreased markedly when the temperature was increased, with a half-life of 5.6 h at 45 °C and a complete inactivation in less than 10 min at 50 °C. The denaturation constant (K_d) increased above 400 times when the pre-incubation temperature was raised from 40 to 50 °C.

Some GH43 can be activated by exogenously supplied divalent cations (Lee et al. 2013). Therefore, the effect of Ca^{2+}, Co^{2+}, Mg^{2+}, Mn^{2+}, Ni^{2+}, and Cu^{2+} on the activity of EcXyl43 was evaluated. Although none of these cations significantly enhanced the catalytic efficiency under optimal conditions (data not shown), the addition of Ca^{2+} improved enzyme stability at 50 °C (Table 3). In the presence of Ca^{2+}, EcXyl43 retained 50% activity after 30 min and the K_d decreased 4-fold compared to the control condition without Ca^{2+}.

The addition of monosaccharides caused modifications in the hydrolysis kinetics of pNPX (Fig. S6), with xylose and arabinose being stronger inhibitors than glucose (Table 4). The enzyme was competitively inhibited by these pentoses with Ki values of 79.9 mM for xylose and 102 mM for arabinose, while glucose was a non-competitive inhibitor (Ki 350 mM). EcXyl43 was relatively tolerant to 5 and 10% ethanol (73 and 52% residual activity, respectively) although activity dropped below 15% in the presence of 20% ethanol (Fig. S7).

Discussion

Glycosyl hydrolases from family 43 comprise a range of activities for aiding the degradation of arabinoxylans. EcXyl43 is the only GH43 from *Enterobacter* sp. that has been expressed and characterized up to date (Campos et al. 2014).

In the current work, it was demonstrated that EcXyl43 is phylogenetically related to β-xylosidases and arabinofuranosidases from this family and clusters with β-xylosidases from lactic acid bacteria. It was predicted to have a catalytic domain with a five-bladed β-propeller fold, the signature structure of GH43 family, linked to a less conserved ancillary C-terminal β-sandwich domain which function has not been fully elucidated yet (Lagaert et al. 2014; Nurizzo et al. 2002).

The active site of other two-domain GH43 β-xylosidases, such as XynB3 and WXyn43, has been previously elucidated (Brux et al. 2006; Falck et al. 2016). They presented a pocket topology, mainly formed by residues from the catalytic domain, and are closed on one side by a loop originated from the ancillary domain. In general, they interact with XOS at two binding subsites (− 1 and + 1). A large number of hydrogen bonds, hydrophobic and stacking interactions hold the glycon xylose in the − 1 subsite, which determines the glycone specificity, while the aglycon-leaving unit is much less tightly bounded to the + 1 subsite (Brux et al. 2006; Falck et al. 2016; Fan et al. 2010). The sequence analysis of EcXyl43 revealed the presence of conserved residues from the catalytic domain involved in xylose recognition and binding to the − 1 subsite, as well as the typical amino acids from the catalytic triad: Asp14 as general base, Glu187 as general acid, and Asp127 as pKa modulator (Brux et al. 2006; Shallom et al. 2005). Not surprisingly, the change of the catalytic amino acid Asp14 by Ala caused the complete inactivation of EcXyl43. Similarly, the activity was lost by mutation of Trp73 (for Gly), which was predicted to be involved in stacking interactions with the substrate. Substitution of the equivalent residue in the arabinase BsArb43A and the bifunctional β-xylosidase/α-L-arabinofuranosidase SXA also caused a significant reduction in their activities (Jordan and Li 2007; Proctor et al. 2005). Trp73 is part of the WAP sequence, invariably conserved among GH43 (Fig. 3), which forms a pocket to guide substrates to bind in the proximity of catalytic residues (Jordan and Li 2007).

Molecular modeling of EcXyl43 also suggested that the β-sandwich ancillary domain forms a loop to bring Phe507 into the active site, a highly conserved residue that also participates in xylobiose binding by stacking interactions (Brux et al. 2006). The lack of activity of the truncated catalytic domain of EcXyl43 could be related to the absence of this loop, which might alter the topology of the active site. However, the replacement of Phe507 by Ala affected the enzymatic activity as much as the elimination of the complete domain. Therefore, this conserved residue would be an essential part of the active site, vital for the activity of EcXyl43 as well as for other β-xylosidases, like Xyl43A from *T. fusca*, as previously reported by Morais et al. (2012). The ancillary C-terminal domain would also play a role in interprotomeric interactions of xylosidases from this family (Falck et al. 2016). In this regard, EcXyl43 was predicted to have a tetrameric structure,

Table 4 Inhibition of EcXyl43 catalysis by monomeric sugars

	Vmax (U/mg prot)	K_M (mM)	Ki (mM)	Inhibition type
pNPX (control)	7.4	10.3	–	–
pNPX + xylose[a]	7.7	22.6	79	Competitive
pNPX + arabinose[a]	7.2	20.6	102	Competitive
pNPX + glucose[a]	5.4	9.7	350	Non competitive

[a] Added at final concentration 100 mM

such as the enzymes BsX (AAB41091), XynB3 (ABI49959), and SXA (AAB97967) from the phylogenetic group IV (Brunzelle et al. 2008; Brüx et al. 2006; Umemoto et al. 2008) (Fig. 1). According to Lagaert et al. (2014), the multimeric quaternary structure may be limited to the enzymes of this group while enzymes from other clusters and clades are monomeric.

EcXyl43 presented clear β-xylosidase activity on linear soluble xylooligosaccharides, and on XOS derived from beechwood xylan, but no arabinofuranosidase activity was detected against arabinoxylan. In this sense, many of the reported GH43 with dual activity have often been characterized with pNPX and pNPA and less frequently with natural substrates (Jordan et al. 2013). The recombinant deAX (ACF39706), isolated from a compost starter mixture and SXA (AAB97967), from *Selenomonas ruminantium*, are among the few GH43 β-xylosidases/arabinofuranosidases tested on natural substrates (Jordan and Li 2007; Wagschal et al. 2009).

The β-xylosidase activity of EcXyl43 was confirmed on X2 to X6, and it was greater when increasing the length of the sugar chain. Contrarily, most β-xylosidases from this family are more active towards X2 than longer XOS (Falck et al. 2016; Jordan et al. 2013; Wagschal et al. 2009). The only GH43 β-xylosidase with an increasing specific activity for X2, X3, and X4 reported to date is BXA43 from *Bifidobacterium animalis* (Viborg et al. 2013), while XylC from the same genus possess similar specificity constants from X2 to X6 (Lagaert et al. 2011). Interestingly, the last two enzymes were placed among the closest to EcXyl43 in evolutionary terms (Fig. 1). The more beneficial turnover of compounds longer than X2 has been related to the presence of additional + 2 (and even + 3 and + 4) subsites in the active site including interactions with the loop from the C-terminal domain (Falck et al. 2016; Viborg et al. 2013). However, the amino acid sequence of this loop is variable among β-xylosidases and the residues involved in such interactions have not been well identified.

The releasing of xylose from short XOS and the absence of transxylosidase activity detected for EcXyl43 indicated that it is a true β-xylosidase operating through an inverting mechanism typical for GH43 enzymes. These enzymes catalyze the hydrolysis of a single residue from the non-reducing end of substrate by inverting the anomeric center involved in the glycosidic bond. The reaction occurs without processivity and, therefore, the hydrolysis products are removed from the active site before initiating another catalytic cycle (Fan et al. 2010). Such hydrolysis mechanism, transxylosylation free, makes inverting β-xylosidases interesting for biomass valorization (Diogo et al. 2014). We demonstrated that the addition of EcXyl43 to xylanases enhanced the hemicellulose deconstruction to fermentable xylose, useful for production of bioethanol and other biotechnological processes. The optimization of enzyme dosage and the incorporation of other biocatalysts could improve the yield in fermentable sugars using minimal enzymatic cocktails containing EcXyl43.

Additionally, thermal stability, tolerance to solvents, and end-product inhibition are some parameters to take into account when developing cost-effective bioprocesses for biomass saccharification. EcXyl43 suffered fast inactivation at 50 °C, similarly to many GH43 xylosidases studied to date (Smaali et al. 2006; Wagschal et al. 2009, 2012). This could mean a disadvantage with respect to thermophilic enzymes, since working above 50 °C reduce the matrix viscosity and consequent mass transport costs as well as microbial contamination risks (Singh et al. 2014). However, the high stability at 40 °C makes it suitable for long-term hydrolysis processes at mesophilic temperatures, which also reduces the energy expenditure during saccharification and avoids lowering the temperature for the subsequent fermentation process.

Interestingly, the addition of Ca^{+2} increased the half-life of EcXyl43 at 50 °C. Ca^{+2} binding sites, which might be involved in its stabilization, were predicted in the structural model. This divalent cation was considered to have a structural and/or a catalytic role in crystallized GH43 that tightly bound Ca^{+2} (Lee et al. 2013). It was suggested that the interaction with metal ions could increase the structural rigidity of some GHs, particularly in connecting loops, and could therefore be related to higher thermal stability (Yeoman et al. 2010).

Pretreated biomass can be enzymatically hydrolyzed either prior to fermentation or in a simultaneous saccharification and fermentation process. The success of an integrated process requires of enzymes resistant to the fermentation conditions (mesophilic temperature, pH around 5) and ethanol. Besides being poorly resistant to acidic conditions (Campos et al. 2014), EcXyl43 was markedly affected by ethanol above 10%, and therefore, its potential for application in SSF/SSCF would be limited. However, the inhibition by monomeric sugars, the final products of the saccharification process, was relatively low if compared with other bacterial and fungal β-xylosidases (Jordan et al. 2013; Saha, 2003; Yang et al. 2014). The competitive inhibition observed for arabinose and xylose and the non-competitive inhibition by glucose could be related with the high specificity for the glycone substrate demonstrated in β-xylosidases GH43 (Brüx et al., 2006). Glucose is not able to occupy the active site due to steric impediments, and consequently, there would be no competition with the substrate for binding sites.

Such moderated inhibition by monomeric sugars, the good stability during long time periods at 40 °C, and the capability for releasing xylose from hemicellulose in combination with xylanases confers to EcXyl43 a great potential as a biocatalyst for saccharification reactions.

Acknowledgments Authors thank MINCYT and CONICET for financial support. OO and FP hold post-doctoral and doctoral fellowships from the Argentinean National Council of Research (CONICET). SG holds an INTA doctoral fellowship. EC, PT, and MC acknowledge CONICET as Research Career members and RM belongs to National Institute of Agriculture Technology (INTA). Pre-treated wheat straw was gently supplied by Dr. Mercedes Ballesteros from CIEMAT, Spain. We thank Igor Polikarpov from USP, Brazil, for critical reading of the manuscript.

Funding This study was funded by projects MINCYT PICT2014-0791 and CONICET PIP2015-11220150100121CO.

Compliance with ethical standards

Conflict of interest Ornella Ontañon declares that she has no conflict of interest. Silvina Ghio declares that she has no conflict of interest. Rubén Marrero Díaz de Villegas declares that he has no conflict of interest. Florencia E Piccinni declares that she has no conflict of interest. Paola M Talia declares that she has no conflict of interest. María L Cerutti declares that she has no conflict of interest. Eleonora Campos declares that she has no conflict of interest.

Ethical approval This article does not contain any studies with human participants or animals performed by any of the authors

References

Brunzelle JS, Jordan DB, McCaslin DR, Olczak A, Wawrzak Z (2008) Structure of the two-subsite β-D-xylosidase from *Selenomonas ruminantium* in complex with 1,3 bis[tris(hydroxymethyl)-methylamino]propane. Arch Biochem Bioph 474:157–166

Brüx C, Ben-David A, Shallom-Shezifi D, Leon M, Niefind K, Shoham G, Shoham Y, Schomburg D (2006) The structure of an inverting GH43 β-xylosidase from *Geobacillus stearothermophilus* with its substrate reveals the role of the three catalytic residues. J Mol Biol 359(1):97–109

Campos E, Negro Alvarez M, di Lorenzo G, Gonzalez S, Rorig M, Talia P, Grasso D, Sáez F, Manzanares Secades P, Ballesteros Perdices M, Cataldi A (2014) Purification and characterization of a GH43 β-xylosidase from *Enterobacter* sp. identified and cloned from forest soil bacteria. Microbiol Res 169(2–3):213–220

Diogo JA, Hoffmam ZB, Zanphorlin LM, Cota J, Machado CB, Wolf LD, Squina F, Dámasio A, Murakami M, Ruller R (2014) Development of a chimeric hemicellulase to enhance the xylose production and thermotolerance. Enzym Microb Technol 69:31–37

Dodd D, Cann IK (2009) Enzymatic deconstruction of xylan for biofuel production. GCB Bioenergy 1(1):2–17

Falck P, Linares-Pastén JA, Adlercreutz P, Karlsson EN (2016) Characterization of a family 43 β-xylosidase from the xylooligosaccharide utilizing putative probiotic *Weissella* sp. strain 92. Glycobiology 26(2):193–202

Fan Z, Yuan L, Jordan DB, Wagschal K, Heng C, Braker JD (2010) Engineering lower inhibitor affinities in β-D-xylosidase. Appl Microbiol Biotechnol 86(4):1099–1113

Ghio S, Ontañon OM, Piccinni FE, Marrero R, Talia P, Grasso DH, Campos E (2018) *Paenibacillus* sp. A59 GH10 and GH11 extracellular Endoxylanases: application in biomass bioconversion. BioEnergy Res 11:174–190

Gírio FM, Fonseca C, Carvalheiro F, Duarte LC, Marques S, Bogel-Łukasik R (2010) Hemicelluloses for fuel ethanol: a review. Bioresour Technol 101(13):4775–4800

Jordan DB, Li XL (2007) Variation in relative substrate specificity of bifunctional β-d-xylosidase/α-l-arabinofuranosidase by single-site mutations: roles of substrate distortion and recognition. Biochim Biophys Acta 1774(9):1192–1198

Jordan DB, Wagschal K, Grigorescu AA, Braker JD (2013) Highly active β-xylosidases of glycoside hydrolase family 43 operating on natural and artificial substrates. Appl Microbiol Biotechnol 97(10):4415–4428

Jørgensen H, Pinelo M (2017) Enzyme recycling in lignocellulosic biorefineries. Biofuels Bioprod Biorefin 11(1):150–167

Lagaert S, Pollet A, Delcour JA, Lavigne R, Courtin CM, Volckaert G (2011) Characterization of two β-xylosidases from *Bifidobacterium adolescentis* and their contribution to the hydrolysis of prebiotic xylooligosaccharides. Appl Microbiol Biotechnol 92(6):1179–1185

Lagaert S, Pollet A, Courtin CM, Volckaert G (2014) β-Xylosidases and α-L-arabinofuranosidases: accessory enzymes for arabinoxylan degradation. Biotechnol Adv 32(2):316–332

Lee CC, Braker JD, Grigorescu AA, Wagschal K, Jordan DB (2013) Divalent metal activation of a GH43 β-xylosidase. Enzym Microb Technol 52(2):84–90

Miller GL, Blum R, Glennon WE, Burton AL (1960) Measurement of carboxymethylcellulase activity. Anal Biochem 1(2):127–132

Morais S, Salama-Alber O, Barak Y, Hadar Y, Wilson DB, Lamed R, Bayer EA (2012) Functional association of catalytic and ancillary modules dictates enzymatic activity in glycoside hydrolase family 43 β-xylosidase. J Biol Chem 287(12):9213–9221

Nurizzo D, Nagy T, Gilbert HJ, Davies GJ (2002) The structural basis for catalysis and specificity of the *Pseudomonas cellulosa* alpha-glucuronidase GlcA67A. Structure 10(4):547–556

Pettersen EF, Goddard TD, Huang CC, Couch GS, Greenblatt DM, Meng EC, Ferrin TE (2004) UCSF chimera-a visualization system for exploratory research and analysis. J Comput Chem 25(13):1605–1612

Proctor MR, Taylor EJ Nurizzo D, Turkenburg JP, Lloyd RM, Vardakou M, Davies GJ, Gilbert HJ (2005) Tailored catalysts for plant cell-wall degradation: redesigning the exo/endo preference of *Cellvibrio japonicus* arabinanase 43A. Proc Natl Acad Sci U S A 102(8):2697–2702

Roy A, Kucukural A, Zhang Y (2010) I-TASSER: a unified platform for automated protein structure and function prediction. Nat Protoc 5(4):725–738

Saha BC (2003) Purification and properties of an extracellular β-xylosidase from a newly isolated *Fusarium proliferatum*. Bioresour Technol 90(1):33–38

Selig MJ, Knoshaug EP, Adney WS, Himmel ME, Decker SR (2008) Synergistic enhancement of cellobiohydrolase performance on pretreated corn Stover by addition of xylanase and esterase activities. Bioresour Technol 99(11):4997–5005

Shallom D, Leon M, Bravman T, Ben-David A, Zaide G, Belakhov V, Shoham G, Schomburg D, Baasov T, Shoham Y (2005) Biochemical characterization and identification of the catalytic residues of a family 43 β-D-xylosidase from *Geobacillus stearothermophilus* T-6. Biochemistry 44(1):387–397

Singh SK, Heng C, Braker JD, Chan VJ, Lee CC, Jordan DB, Yuan L, Wagschal K (2014) Directed evolution of GH43 β-xylosidase XylBH43 thermal stability and L186 saturation mutagenesis. J Ind Microbiol Biotechnol 41(3):489–498

Smaali I, Rémond C, O'Donohue MJ (2006) Expression in *Escherichia coli* and characterization of β-xylosidases GH39 and GH-43 from *Bacillus halodurans* C-125. Appl Microbiol Biotechnol 73(3):582–590

Tamura K, Stecher G, Peterson D, Filipski A, Kumar S (2013) MEGA6: molecular evolutionary genetics analysis version 6.0. Mol Biol Evol 30(12):2725–2729

Umemoto Y, Onishi R, Araki T (2008) Cloning of a novel gene encoding β-1,3-xylosidase from a marine bacterium, *Vibrio* sp. strain XY-214, and characterization of the gene product. Appl Environ Microbiol 74:305–308

Viborg AH, Sørensen KI, Gilad O, Steen-Jensen DB, Dilokpimol A, Jacobsen S, Svensson B (2013) Biochemical and kinetic

characterisation of a novel xylooligosaccharide-upregulated GH43 β-D-xylosidase/α-L-arabinofuranosidase (BXA43) from the probiotic *Bifidobacterium animalis* subsp. lactis BB-12. AMB Express 3(1):56

Wagschal K, Heng C, Lee CC, Wong DW (2009) Biochemical characterization of a novel dual-function arabinofuranosidase/xylosidase isolated from a compost starter mixture. Appl Microbiol Biotechnol 81(5):855–863

Wagschal K, Jordan B, Braker JD (2012) Catalytic properties of β-D-xylosidase XylBH43 from *Bacillus halodurans* C-125 and mutant XylBH43-W147G. Process Biochem 47(3):366–372

Yang X, Shi P, Huang H, Luo H, Wang Y, Zhang W, Yao B (2014) Two xylose-tolerant GH43 bifunctional β-xylosidase/α-arabinosidases and one GH11 xylanase from *Humicola insolens* and their synergy in the degradation of xylan. Food Chem 148:381–387

Yang J, Yan R, Roy A, Xu D, Poisson J, Zhang Y (2015) The I-TASSER suite: protein structure and function prediction. Nat Methods 12(1):7–8

Yeoman CJ, Han Y, Dodd D, Schroeder CM, Mackie RI, Cann IK (2010) Thermostable enzymes as biocatalysts in the biofuel industry. Adv Appl Microbiol 70:1–55